Long-term nitrogen addition suppresses microbial degradation, enhances soil carbon storage, and alters the molecular composition of soil organic matter

Jun-Jian Wang[a†], Richard D. Bowden[b], Kate Lajtha[c], Susan E. Washko[b‡], Sarah J. Wurzbacher[b§], and Myrna J. Simpson[a,*]

[a]Environmental NMR Centre and Department of Physical and Environmental Sciences, University of Toronto Scarborough, 1265 Military Trail, Toronto, ON M1C 1A4, Canada.

[b]Department of Environmental Science, Allegheny College, Meadville, PA 16335, USA.

[c]College of Crop and Soil Science, Oregon State University, Corvallis, OR 97331, USA.

[†]Present address: School of Environmental Science and Engineering, Guangdong Provincial Key Laboratory of Soil and Groundwater Pollution Control, Southern University of Science and Technology, Shenzhen, Guangdong 518055, China.

[‡]Present address: School of Natural Resources and the Environment, University of Arizona, Tucson, AZ, 85721, USA.

[§]Present address: Penn State Extension, The Pennsylvania State University, University Park, PA 16802, USA.

*Corresponding Author, Tel.:416-287-7234; Fax: 416-287-7279; e-mail: myrna.simpson@utoronto.ca (M.J. Simpson)

Key Words: forest soil, carbon storage, carbon biogeochemistry, phospholipid fatty acids, organic matter biomarkers, lignin, cutin, suberin, forest soils.

Abstract

Forest soil organic carbon (SOC) is one of the largest reservoirs of terrestrial carbon (C) and is a major component of the global C cycle. Yet there is still uncertainty regarding how ecosystems, and the SOC they store, will respond to changes due to anthropogenic processes. Current and future reactive nitrogen (N) deposition to forest soils may alter biogeochemical processes and shift both the quantity and quality of stored SOC. We studied SOC storage and molecular-level composition after 22 years of N additions (100 kg N ha^{-1} yr^{-1}) in a temperate deciduous forest. SOC storage in surface soils increased by 0.93 kg m^{-2} due to a decline in microbial biomass (phospholipid fatty acids) and litter decomposition. N additions resulted in the selective preservation of a range of plant-derived compounds including steroids, lignin-derived, cutin-derived, and suberin-derived compounds that have anti-microbial properties or are non-preferred microbial substrates. This overall shift in SOC composition suggests limited sustainability and a decline in soil health. The reduction in microbial biomass and increase in specific SOC components demonstrate that long-term N fertilization negatively alters fundamental C cycling in forest soils. This study also demonstrates unequivocally that anthropogenic impacts C and N cycling in forests at the molecular-level and must be considered more holistically.

Introduction

Forest soil organic carbon (SOC) is one of the largest terrestrial carbon (C) pools (~383 × 10^{15} g; Pan et al. 2011) that regulates global and regional C, nutrient and pollutant cycling, and controls C feedback to climate change (Schmidt et al. 2011; Lehmann and Kleber 2015). Soil C dynamics are strongly coupled to nitrogen (N) cycling, and the prolific use of fertilizers and fossil fuels has increased reactive N deposition globally (~150 × 10^{12} g yr^{-1}) into soils (Lamarque 2005;

Galloway et al. 2008) well above pre-industrial levels. Although there has been a reduction in N emissions and deposition in much of Europe and the United States (Waldner et al., 2014, Li et al. 2016), with resulting decreases in wet deposition (Du et al. 2014), large increases in N deposition rates are observed in other regions, particularly in Asia (Vet et al., 2014). Furthermore, increasing deposition of reduced nitrogen forms indicate that atmospheric deposition of nitrogen will continue to result in ecosystem-level inputs that exceed critical loads to forest ecosystems (Pardo et al. 2015).

It is currently unclear how and to what extent long-term N inputs to soils from anthropogenic processes will alter forest SOC storage and C biogeochemical cycling (Aber et al. 1998; Gallo et al. 2005; Zak et al. 2017) and consequently alter ecosystem services. To date, studies have reported varying results, with N additions increasing, decreasing or causing no change in forest SOC storage (Janssens et al. 2010; Lu et al. 2011; Frey et al. 2014; Yue et al. 2016). SOC content and composition is controlled mainly by both plant inputs and microbial processing and degradation of SOC (Schmidt et al. 2011; Lehmann and Kleber 2015). Although N fertilization can stimulate plant growth and increase litterfall (Yue et al. 2016), it can also accelerate or slow down microbial processing of plant residues (Hobbie et al. 2012; Xia et al. 2017), thus altering SOC chemistry. Given the complexity of C cycling processes that influence soil biogeochemistry, and the importance of C chemistry in controlling nutrient availability, providing energy to soil micro- and macro-biota, and in regulating soil C sequestration, there is a critical need to use sensitive chemical characterization methods to understand how long-term N deposition may alter the molecular-level composition of SOC and biogeochemical controls on SOC accrual and turnover (Schmidt et al. 2011; Lehmann and Kleber 2015). Furthermore, responses of SOC to N additions are to date derived mostly from relatively short-term N-fertilization experiments (<10 years of treatment) or limited types of SOC investigations (Feng et al. 2010; Liu et al., 2016; Pisani,

et al. 2015; Wu et al. 2015; Zak et al. 2017). Here, we hypothesize that there are indeed compound-specific SOC responses to long-term N fertilization that depend on the initial molecular size, source, and turnover of SOC. To test this hypothesis, we quantified SOC storage and composition with soil depth after 22 years of N fertilization (100 kg N ha^{-1} yr^{-1} as of NH_4NO_3) in a temperate deciduous forest in Meadville, Pennsylvania, USA. A range of sensitive and targeted microbial- and plant-derived compounds were analyzed in O, A and B horizons. This included the isolation and quantification of lipids and other small molecules as well as compounds derived from cutin, suberin and lignin as well as microbial-specific phospholipid fatty acids (PLFAs) using gas chromatography-mass spectrometry (GC-MS). In addition, non-targeted solid-state ^{13}C nuclear magnetic resonance (NMR) spectroscopy was used to measure potential shifts in the overall SOC composition.

Materials and Methods

Site description and soil sampling

The nitrogen (N) fertilization experiment at the Allegheny College Bousson Environmental Research Reserve in northwestern Pennsylvania (41°36'N, 80°2'W) was started in 1994. This 80-year-old forest is a N-rich site dominated by black cherry (*Prunus serotina*; 60% of the aboveground biomass) and sugar maple (*Acer saccharum*; 28% of the aboveground biomass (Bowden et al. 2000; Chan et al. 2005)). Litterfall is 2.1 Mg C ha^{-1} $year^{-1}$ and total soil N (to 60 cm) is about 10,000 kg N ha^{-1}. The soils are Alfisols (a silty-loam texture) and are moderately well drained with a bulk density of 0.52±0.01 g cm^{-3}, pH of 4.0 and a cation exchange capacity of 3.73 $cmol_c$ kg^{-1} in the upper 15 cm of the mineral soil. Alfisols cover 13.5% of ice-free land area and contain 8% of soil C globally (Eswaran et al. 1993; Pries et al. 2017). We do not see invasive, non-native earthworms at the site, either at the surface or in soil pits.

There are three control and three N-fertilized 15 x 15 m plots. Ammonium nitrate (NH_4NO_3) is added in six aqueous additions using a backpack sprayer during the growing season, from May/June through August/September each year with an annual rate of 100 kg N ha^{-1} yr^{-1} (Bowden et al. 2000). The application rate was selected to 1) accelerate atmospheric N deposition and examine potential changes in forest responses to long-term N deposition, and 2) be comparable to addition rates in a similar N-addition study at the Harvard Forest Long-Term Ecological Research site (Bowden et al. 1990). When the study was initiated (1994) total inorganic wet N deposition was 6.1 kg N ha^{-1} yr^{-1} in Kane, PA and 100 5.3 kg N ha^{-1} yr^{-1} in Chautauqua, NY (NADP 2018), with about 35% of N being deposited as NH_4 and 65% as NO_3. Interpolating NADP maps of total wet plus dry deposition indicated that total N deposition at Bousson in 2000 was between 16 and 18 kg N ha^{-1} yr^{-1}. More recently (2017), total wet inorganic deposition in Kane is 4.8 kg N ha^{-1} yr^{-1} (55% NH_4, 45% NO_3) and total wet plus dry deposition (2016) is between 12 and 14 kg N ha^{-1} yr^{-1} (NADP 2018). Over the course of the study, sulfate and H^+ deposition have also declined dramatically (NADP 2018).

After surface litter removal, soils from O horizon (depth of approximately 1–3 cm), A horizon (depth of approximately 3–8 cm), and top 10 cm of the B horizon were collected from two 20×20-cm-area soil blocks within each plot on May 9, 2016. Therefore, six soil blocks (two blocks in each of the three plots) were collected from both control and N-fertilized plots and they were analyzed individually. All samples were sieved (2 mm), lyophilized, ground with a ball mill before chemical analyses. The dried mass of each horizon of each soil block was weighed and recorded. Soil pH (determined in deionized water) after 21 years of N amendment indicated a slight decline in both the O and A horizons (unpublished data). With N addition, soil pH decreased from 4.19 ±

114 0.31 (control plots) to 3.69 ± 0.13 (N amended plots) in the O horizon and from 3.97 ± 0.31 (control
115 plots) to 3.54 ± 0.08 (N amended plots).
116
117 Total carbon (C) and nitrogen (N) and soil fractionation
118 The total C and N contents in soils were determined with a Thermo Flash 2000 elemental
119 analyzer. A subset of mineral soil samples (A and B horizons) were fractioned by density using
120 sodium polytungstate following Sollins et al. (2006) and divided into three pools including light
121 (<1.85 g cm^{-3}), aggregate (1.85–2.4 g cm^{-3}), and heavy (>2.4 g cm^{-3}) fractions (Hatton et al. 2012).
122
123 Biomass production and decomposition
124 Litterfall was collected monthly from two 1.0 m^2 litter collectors on each plot and dried at
125 105 ºC for 48 h. Three 15×15-cm-area soil samples from each plot for root mass analysis were
126 collected in autumn of 2010 in the manner described previously (Bowden et al. 2014), with the
127 exception that the B-horizon soils were collected using a gas-powered 9.62-cm diameter diamond-
128 bit stainless steel soil corer (Earthquake, 9800B). Roots (0-1 mm dia.) were removed from each
129 soil sample by hand, and dried at 105 ºC for 48 h. Aboveground tree growth was estimated by
130 measuring tree diameters at 1.35 m, and applying species-specific biomass equations (Tritton and
131 Hornbeck 1982) for each of the trees on the plots.
132 Leaf litter samples for decomposition estimates were collected from 9 m^2 catchment
133 screens placed in the middle of each nitrogen addition plot and on the outside edge of each control
134 plot and were homogenized by treatment. Leaf pack composition for mixed litter bags was
135 determined through an autumnal collection in 2014 of litter caught in two 1.0 m^2 screens per plot,
136 dried for 48 h at 105 °C, and sorted to species. Litter bags (20×30 cm for leaves, 0.18 mm^2 mesh

137 no-see-um netting) contained the air-dried equivalent of 2.0 g of 105 ºC -dried leaf litter. Four bags
138 for each of black cherry (*Prunus serotina*), sugar maple (*Acer saccharum*), or mixed leaf litter
139 (53.8% sugar maple, 29.5% black cherry, 16.7% beech (*Fagus grandifolia*)) were deployed per
140 plot in each treatment, in mid-October 2015, the time of maximum autumnal litterfall. Litter bags
141 were placed directly atop the O horizon and were buried under the leaves. Bags were collected in
142 October of the following year; litter was oven-dried for 48 hours at 105°C and weighted.
143
144 Targeted organic matter compound analysis by gas chromatography-mass spectrometry (GC-MS)
145 Specific organic matter compounds with various microbial- and plant-derived sources were
146 isolated and quantified using GC-MS. Phospholipid fatty acids (PLFAs) were extracted by a
147 modified Bligh-Dyer method and analyzed by GC-MS (Frostegård and Bååth 1996). Briefly, 0.5-
148 2.5 g soil samples (depending on the C content) were extracted using 16 mL of methanol, 8 mL of
149 chloroform, and 6 mL of 0.15 M sodium citrate buffer (acidified to pH = 4). The lipid extract in
150 $CHCl_3$ phase was collected after centrifugation and separation. The lipid extract was then
151 fractionated into neutral, glycol, and polar lipids with 10 ml of $CHCl_3$, 20 ml of acetone, and 10
152 ml of CH_3OH, respectively by silica column chromatography. The PLFA in the polar fraction was
153 concentrated, dried by N_2 gas, and derivatized into methyl esters. The methyl esters were extracted
154 with 5 mL of hexane and chloroform mixture (4:1, v/v) three times, dried under N_2 gas in a 2 mL
155 glass vial. Extracts were derivatized prior to analysis by GC-MS (Feng and Simpson 2009).
156 Acyclic lipids, plant-derived steroids, sugars, as well as the cutin-, suberin-, and lignin-
157 derived compounds were sequentially extracted by dichloromethane/methanol extraction, base
158 hydrolysis and CuO oxidation, respectively and analyzed by GC-MS using established methods
159 (Otto and Simpson 2007; Otto et al. 2005). First, 0.1-1.0 g of soil sample (depending on the C

content) was sonicated with 30 mL dichloromethane, dichloromethane and methanol mixture (1:1, v:v), and methanol (each for 15 min). The combined solvent extracts were then filtered through Whatman GF/A and GF/F glass filters, concentrated by rotary evaporation, and dried by N_2 gas in a 2 mL glass vial. Second, the solvent-extraction residues were air dried and base hydrolyzed with 20 mL of 1 M methanolic KOH at 100 °C for 3 h. The extracts were sonicated twice with 15 ml dichloromethane:methanol (1:1, v:v), centrifuged and acidified to pH 1. The combined supernatants were rotary evaporated, and the hydrolysable lipids were liquid-liquid extracted three times with 30 ml diethyl ether. The extracts were dried with Na_2SO_4, concentrated by rotary evaporation, and dried by N_2 gas in a 2 mL glass vial. Finally, the base hydrolyzed residues were air dried and oxidized with 1 g CuO, 100 mg ammonium iron (II) sulfate hexahydrate [$Fe(NH_4)_2(SO_4)_2 \cdot 6H_2O$] and 15 mL of 2 M NaOH in Teflon lined bombs at 170 °C for 2.5 h. The extracts were acidified to pH=1 and kept for 1 h at room temperature in the dark to prevent the polymerization of cinnamic acids. Then, the supernatants were solid-phase extracted using HLB cartridges and dried with anhydrous Na_2SO_4. The extracts were concentrated by rotary evaporation and dried by N_2 gas in a 2 mL glass vial and then derivatized prior to GC-MS analysis (Otto and Simpson 2007; Otto and Simpson 2006).

All compounds were analyzed by GC-MS using an Agilent 7890B gas chromatograph equipped with a 5977B mass spectrometer with electron impact (70 eV) ionization. Samples (1 μL) were injected at an inlet temperature of 280 °C onto a HP-5MS fused silica capillary column (30 m × 0.25 mm i.d. × 0.25 μm film thickness). The oven temperature program was: 65 °C for 2 minutes, followed by an increase of 6 °C min^{-1} to 300 °C, followed by a 20 minute isothermal hold. The carrier gas (helium) flow rate was 1 mL min^{-1}. Data acquisition was performed using Agilent Mass Hunter GC-MS Acquisition (version B.07.03.2129) and data were processed using Agilent

Enhanced ChemStation software (version E.02.02.1431). External standards were used for quantification: tetracosane (analytical standard grade, Sigma-Aldrich), 1-docosanol (approximately 98%, Sigma-Aldrich), methyl tricosanoate (analytical standard grade, Fluka Analytics) and ergosterol (>75%, Sigma-Aldrich) for solvent extracts; methyl tricosanoate for base hydrolysis products; and syringic acid (minimum 98%, Sigma-Aldrich) and syringaldehyde (98%, Sigma-Aldrich) for copper oxidation products. Compounds were identified using Wiley Registry (9^{th} edition) plus NIST (2008) mass spectral databases, mass spectral library of soil compounds, and published mass spectra. Mean and standard errors of six replicates were calculated for each soil horizon of either the control or N-fertilized plots.

Solid-state ^{13}C nuclear magnetic resonance (NMR) analysis

Solid-state ^{13}C nuclear magnetic resonance (NMR) analysis was performed to assess changes in C chemistry. The mineral soil samples from A and B horizons were repeatedly extracted with hydrofluoric acid (0.3 M), rinsed with deionized water, and lyophilized to concentrate the organic matter for better detection by ^{13}C NMR (Schmidt et al. 1997). The soils from O horizon and HF-washed soils from A and B horizons were characterized by solid-state ^{13}C cross polarization magic angle spinning (CPMAS) NMR. Solid-state ^{13}C NMR spectra were collected using a 500 MHz Bruker BioSpin Avance III spectrometer equipped with a 4 mm H-X MAS probe, using a ramp-cross-polarization pulse program with a spinning rate of 11 kHz, a contact time of 1 ms, and a recycle delay of 1 s (Conte et al. 2004). Four regions of the ^{13}C NMR spectra were defined and calculated for their relative abundance (Baldock et al. 1992): 1) alkyl C (0-50 ppm; from cutin, suberin, lignin, lipids, and amino acid side chains), *O*-alkyl C (50-110 ppm; from carbohydrates, peptides, and methoxyl C in lignin), aromatic + phenolic C (110-165 ppm;

206 from lignin and amino acids found in peptides), and carboxyl + carbonyl C (165-210 ppm; from
207 fatty acids and peptides).
208
209 Statistical analyses
210 One and two-way analyses of variance (ANOVA) with Tukey's posthoc comparison were
211 used to examine the main and interactive effects of N fertilization and soil horizon on the soil
212 chemical properties (i.e., C and N contents and concentrations and/or ratios of SOC components)
213 and effects of N on litter decomposition. Root litter mass change after one year was assessed with
214 a paired *t*-test. Because the N fertilization often interacted with the soil horizon to affect the soil
215 chemical properties, analyses of simple main effects for N fertilization in each soil horizon were
216 also conducted. The main and simple main effects of N fertilization were considered as significant
217 when $P < 0.05$. Two-tailed Pearson correlations were conducted to explore the relationships among
218 soil chemical properties. Detailed data and statistical results are available in Tables S4-S6.
219
220 **Results**
221 Total carbon (C) and nitrogen (N) and soil density fractions
222 With long-term N-fertilization, total soil C content increased significantly in both the O
223 and A horizons respectively (Table 1). Total N content did not significantly differ in all soil
224 horizons (Table 1). As such, the N-additions only impacted total soil C content in this forest, but
225 we could not detect a change in soil N content. In the O horizon, total soil C content increased
226 from 22.2% to 30.2% with N-addition relative to the control plots. In the A horizon, soil C content
227 increased from 6.77% (control) to 10.06% with N-fertilization. Soil C content did not change
228 significantly in the B horizon (Table 1). Soil C storage in each horizon was calculated from the

229 product of soil C content (with units converted from % to kg-C kg-soil^{-1}) and the soil mass of a
230 horizon (in kg-soil m^{-2}). Overall soil C storage in the O, A, and B horizons increased 17%, from
231 5.32±0.71 kg m^{-2} in the control plots to 6.25±0.34 kg m^{-2} in the N-fertilized plots (P=0.27; Fig. 1).
232 Soil C storage (in kg-C m^{-2}) increases were horizon-specific as most of the accrual occurred in the
233 O horizon (an increase of 90% compared to the control; P=0.001), followed by the A (+11%;
234 P=0.64) and B (+6%; P=0.66) horizons (Fig. 1 and Table 2).
235 Both A and B horizons were separated into density fractions to determine any changes in
236 C distribution amongst different pools with long-term N-addition. The light fraction increased
237 significantly in the A horizon and contained more than twice as much C compared to the control
238 (Fig. 2). This shift in C distribution indicates that more plant-derived C accumulated in the light
239 fraction with long-term N-enrichment. The distribution in soil C did not change significantly
240 amongst the other density fractions in either the A or B horizon (Fig. 2) demonstrated that long-
241 term N-fertilization impacted the processing of plant-derived inputs.
242
243 Biomass production and decomposition
244 Litterfall and root biomass were monitored to determine changes in plant-derived inputs
245 with N-enrichment (Fig. 3). Interestingly, no significant differences were observed in litterfall flux,
246 aboveground production, and fine root mass in the O and A horizon (Fig. 3). Fine root mass was
247 observed to increase in the B horizon (Fig. 3) indicating the potential for increased root-derived
248 inputs deeper within the profile. The mass remaining after 1 year of litter decomposition for black
249 cherry leaf litter, sugar maple leaf litter, and mixed leaf litter was 69.7%±1.8%, 84.6%±0.9%, and
250 72.0%±1.1%, respectively. With N addition, the corresponding values increased to 74.0%±1.3%,
251 89.3%±0.7%, and 79.7%±1.0%, respectively. Clearly, litter decomposition was reduced

252 significantly with N-fertilization (Fig. 4). This reduction in decomposition did not vary with litter
253 type (Fig. 4).
254
255 Targeted organic matter compound analysis by gas chromatography-mass spectrometry (GC-MS)
256 Total PLFA concentrations (Fig. 5) significantly decreased in both O and A horizons
257 indicating a reduction in microbial biomass with N-fertilization. The concentration of PLFAs also
258 declined in the B horizon but not significantly (Fig. 5). With N-enrichment, the distribution of
259 gram-negative, gram-positive and fungal PLFAs was also altered and all three microbial classes
260 declined markedly (Fig. 5). When bacteria are faced with substrate constraints or other stresses
261 such as drought, they produce more of the cyclopropane PLFAs as compared to the
262 monounsaturated versions (Bossio and Scow 1998; Feng and Simpson 2009). A ratio of these
263 PLFAs (cy17:0/16:1ω7c and cy19:0/18:1ω7c) can be compared to ascertain the degree of stress
264 exhibited by microbes. These ratios increased significantly with N-fertilization (Fig. 5) suggesting
265 that microbial stress was enhanced with long-term N-addition.
266 Several targeted organic matter compounds shifted with long-term N-enrichment (Fig. 6;
267 Table 2). Plant-derived steroids, lignin-derived, cutin-derived compounds, acyclic lipids, suberin-
268 derived compounds and simple sugars all exhibited changes in their concentration and storage but
269 to varying extents and depending on soil depth. Plant-derived steroids, which include (β-sitosterol,
270 stigmasterol, sitosterone, stigmasta-3,5-dien-7-one, and campesterol, increased markedly (+132%)
271 and more so than other plant-derived compounds (Fig. 6; Table 2). Significant increases were also
272 observed for lignin-, cutin-, and suberin-derived compounds in the O horizon. The storage of
273 specific organic matter compounds was also altered in the A and B horizons but not significantly.
274

Solid-state ^{13}C nuclear magnetic resonance (NMR) analysis

Solid-state ^{13}C NMR spectroscopy provides an overview of soil organic matter composition but lacks the sensitivity of targeted compound analysis (Simpson and Simpson 2012). The distribution of various organic matter classes is listed in Table 1. In each soil horizon, only small or no differences were observed in each of the compound class group. The most dominant group was the *O*-alkyl region (50-110 ppm) which contains resonances mostly from carbohydrates and peptides but may have contributions from lignin (methoxyl group; (Preston et al. 1997)). Alkyl-C did not vary with N-fertilization, likely reflecting small changes in plant-derived waxes and other lipids. Similarly, the aromatic and phenolic C and carboxyl and carbonyl C regions did not exhibit major differences with N-enrichment. The alkyl/*O*-alkyl C ratio is used to assess the relative degradation stage of organic matter because as oxidative degradation increases, the resonances from more labile compounds will result in a decrease in the *O*-alkyl signal intensity. These ratios (Table 1) for the A and B horizon were similar and did not provide evidence for any differences in the relative degradation state of organic matter in these horizons. The O horizon reflected a small difference in the alkyl/*O*-alkyl ratio but this is likely due to the difference in *O*-alkyl C in this horizon. It is important to note that the error associated with this type of NMR analysis for relative comparisons of different organic matter classes is ~5% (Dria et al. 2002) and indicates that for these samples, solid-state ^{13}C NMR lacks the ability to detect changes in organic matter composition.

Discussion

Impacts on soil organic carbon (SOC) storage and microbial biomass

297 We observed significant increases in SOC storage in the entire soil profile (O, A and B
298 horizons) after 22 years of N fertilization. Increases in soil C sequestration have been linked to
299 increased litterfall inputs at the soil surface, because N fertilization may increase plant productivity
300 (Aber et al. 1998; Frey et al. 2014). However, litterfall (2010-2016) in the Control plots was
301 492±42 g m^{-2} y^{-1}, compared to 478±35 g m^{-2} y^{-1} in the N-fertilized plots (Fig. 3) indicating that
302 aboveground inputs were not enhanced by N fertilization. Additionally, there was no increase in
303 growth rates of aboveground biomass (2005-2009) between the control plots (7.9±1.0 Mg ha^{-1} y^{-1})
304 and the fertilized plots (7.3±3.7 Mg ha^{-1} y^{-1}; Fig. 3). Interestingly, our study at this same forest
305 that experimentally doubled the annual aboveground litterfall inputs for 20 years did not observe
306 any net gain in soil C storage, because additional plant inputs were decomposed by soil microbiota
307 (Wang et al. 2017). This companion study reported a small decrease in SOC with doubling of
308 aboveground inputs and this was attributed to enhanced decomposition, likely due to soil priming,
309 of these additional inputs (Wang et al. 2017).
310 We also did not find significant differences in standing root biomass between control and
311 N-fertilized plots at O and A horizons, although we do not know how root productivity or turnover
312 compared between the treatments (Fig. 3). Therefore, aboveground or belowground plant inputs
313 alone are unlikely to have contributed to the large gains in SOC storage in the O and A horizons.
314 Because SOC in the O horizon is mainly from partially decomposed plant residues, the +90% SOC
315 accrual is most likely caused by a reduction in SOC processing. To examine this further, soil
316 density fractions were isolated because the light fraction is typically an indicator of plant-derived
317 compounds that are not as degraded as SOC found in the mineral fractions (Sollins et al. 2009).
318 In the A horizon, there was a higher mass of light fraction (density < 1.85 g m^{-3}; mainly derived
319 from plant residues) in N-fertilized plots (43.52 ± 3.34 mg C/g soil) than the control plots (19.58

± 11.52 mg C/g soil; Fig. 2), suggesting that the plant-derived inputs were less decomposed. This is consistent with observations reported in other studies where N amendments decreased SOC degradation (Frey et al. 2014; Li et al. 2017).

The combined observations of increased SOC storage, no significant changes in litterfall, and an increase in the light fraction with N fertilization (Figs. 1-3) collectively suggest a decline in microbial degradation of soil organic matter. Several studies have demonstrated that N addition to soil can reduce microbial biomass and alter microbial diversity (Feng et al. 2010; Frey et al. 2014; Morrison et al., 2016; Pisani et al. 2015; Ramirez et al. 2012). We therefore measured microbial PLFAs, which are excellent indicators of microbial biomass and microbial community structure (Bossio and Scow 1998; Feng and Simpson 2009; Frostegård and Bååth 1996; Zelles et al. 1995). With N fertilization, PLFA concentrations declined markedly in the O and A horizons (Figs. 5). The decline in PLFA concentrations indicates a reduction in microbial biomass with N fertilization that likely resulted in increased SOC storage. When facing substrate constraints, drought or changes in temperature, bacteria increase production of cyclopropane PLFAs and decrease production of monounsaturated PLFAs (Bossio and Scow 1998; Feng and Simpson 2009). We observed that ratios of cyclopropane PLFAs to their monounsaturated precursors (cy17:0/16:1ω7c and cy19:0/18:1ω7c) and the ratio of total saturated to total monounsaturated PLFAs increased for all soil horizons (all $P<0.01$; Fig. 4 and Table S1) indicating that in addition to a decline in total microbial biomass, microbes were under stress with long-term N fertilization. Short-chain ($<C_{20}$) acyclic lipids (including *n*-alkanes, *n*-alkanols, and *n*-alkanoic acids) which are predominantly microbially-derived (Otto et al. 2005), also decreased in O and A horizons (Table S1). Consequently, our data indicate that both biomass and subsequent microbially-derived inputs declined with long-term N fertilization. Furthermore, the observed decrease in PLFA

concentrations in O and A horizons in our study is greater than decreases reported from most short-term fertilization studies (Liu et al. 2016), supporting the hypothesis that bacterial and fungal biomass continue to decline with long-term N fertilization (Treseder 2008). A shift in microbial community composition was also observed with N-fertilization (Fig. 5 and Table S1) in conjunction with decreases in bacteria (both gram-negative and gram-positive), fungi, and actinomycetes. Other studies have also reported altered microbial community composition with N fertilization (Allison et al. 2008; Bhatnagar et al. 2018) Although the localized physiological mechanisms are not well understood (Treseder 2008), our results clearly demonstrate marked alterations to the microbial community composition and reduced active microbial biomass in O and A horizons with long-term N fertilization (Frey et al. 2014). These upper layers of soil are where microbial communities thrive and are most active in degradation of plant-derived inputs. Although plant litter inputs did not increase in surface soils with N fertilization, the one-year leaf litter decomposition, both in single and mixed assemblages, was significantly reduced by N fertilization (P<0.001; Fig. 4). Therefore, multiple observations collectively support that the reduced microbial biomass and likely reduced microbial processing of SOC resulted in higher SOC storage with N fertilization.

Selective preservation of specific soil organic carbon (SOC) components

The suppression of SOC microbial processing also resulted in a large shift in SOC composition and the concentration of specific SOC components (Fig. 6). Plant-derived steroids (β-sitosterol, stigmasterol, sitosterone, stigmasta-3,5-dien-7-one, and campesterol) increased more than all other studied plant-derived compounds (Fig. 6). Storage of plant-derived steroids increased by 4.57 g m^{-2}, with increases of +281%, +103%, and +50% in O, A, and B horizons, respectively

(Fig. 6). Summed across the three horizons, the three measured steroids increased by 132% (P=0.02). The more complex plant biopolymers (e.g., lignin and acid insoluble fraction of plant residues) have been observed to be retained preferentially compared to small extractable molecules during litter decomposition with N addition (Xia et al. 2017). However, we found that plant-derived steroids, although small molecules, have the greatest percentage increase in storage and contribute significantly to the SOC accrual. This suggests that the component-specific SOC response to long-term N fertilization is not necessarily a result of the molecular size of the SOC components or the hypothesized chemical recalcitrance of plant-derived compounds. More importantly, these plant-derived steroids represent the largest group of plant secondary compounds and may have antibacterial and antifungal properties (Smania et al. 2003; Adamczyk et al. 2015). Their concentrations correlated significantly with the SOC content and with indicators of microbial composition (e.g., fungal/bacterial PLFA ratio) and microbial stress indicators (e.g., cy17:0/16:1ω7c; two-tailed Pearson's, all $P<0.01$; Figs. S2 and S3). Taken collectively, our results suggest a new hypothesis wherein accumulation of plant-derived steroids in N-fertilized plots may have suppressed microbial biomass, thus decreasing organic matter decomposition, and subsequently increasing soil C sequestration.

Lignin is the second largest form of plant-derived C after cellulose and a major contributor of aromatic and phenolic components in soils (Kögel-Knabner 2002; Bianchi 2011). Lignin-derived phenols (including ether-bound vanillyl, syringyl, and cinnamyl phenolics) also increased significantly (+94% in total; $P=0.01$; Fig. 6) with N fertilization. As with the plant-derived steroids, accrual of lignin-derived phenols occurred in all soil horizons and was most significant in the O horizon (Fig. 6). The lignin oxidation indicators, i.e., lignin-derived acid to aldehyde ratios of vanillyls and syringyl (Hedges et al. 1988), did not significantly increase with N fertilization in

any horizon (Table S1). This observation, together with the overall reduced microbial biomass, demonstrates that lignin oxidation was suppressed with N fertilization. In addition, the slightly increased aromatic and phenolic C in the NMR spectra (Table 1), mainly originating from lignin and amino acids of peptides (Baldock et al. 1992; Preston et al. 1997), further confirms the increased preservation of lignin in all soil horizons. The concentration of lignin-derived phenols in previously studied N-fertilized soils has shown a range of responses, including increases (Frey et al. 2014), decreases (Pisani et al. 2015), and significant alterations (Feng et al. 2010; Theuerl et al., 2010; Wu et al., 2015), possibly due to site-specific alteration in microbial community. A recent meta-analysis suggested that short-term increases of lignin-derived phenols to N fertilization seem to diminish with longer-term N fertilization (Liu et al. 2016), and no significant increase in lignin phenols was found in longer-term (14.5 and 16 years) N-fertilized forests (Theuerl et al. 2010; Thomas et al. 2012). Our results from longer N fertilization strongly support SOC accrual with significant contributions from lignin. As with the concentrations of plant-derived steroids, the concentrations of lignin-derived phenols correlated significantly with the SOC content and microbial indicators (two-tailed Pearson's, all $P<0.1$; Fig. S2) further suggesting that lignin preservation is directly connected to our other observations.

The cutin- and suberin-derived compounds are valuable indicators for understanding the relative contributions of aboveground and belowground plant inputs to soil (Angst et al. 2016; Crow et al. 2009; Otto and Simpson 2006). The storage and accumulation of cutin-derived compounds increased (+59%) more than suberin-derived compounds (+15%; Fig. 6). This resulted in an increase in the cutin to suberin ratio in N-fertilized soils ($P_{\text{O-horizon}}=0.06$; Table S1). Hence, N fertilization increased contributions from aboveground plant C more than contributions from belowground plant C. Thus, the compositional shift in SOC retains more of a signature

412 characteristic of aboveground plant inputs over belowground inputs in N-rich forests (Wu et al.
413 2015; Peng et al. 2017). Similarly, the long-chain acyclic lipids (≥C_{20}; including *n*-alkanes, *n*-
414 alkanols, and *n*-alkanoic acids; mainly derived from aboveground plant inputs in this forest (Wang
415 et al. 2017) also showed higher accrual compared to the suberin-derived compounds (Fig. 6). This
416 observation further supports the shift of SOC composition to higher contributions from
417 aboveground inputs. In addition, the alkyl C in the NMR spectra, mainly originating from plant
418 cutin, suberin, waxes, and microbe-derived lipids in the soil, was slightly higher in N-fertilized
419 plots than the controls for O horizon but was similar between control and N-fertilized plots for A
420 and B horizons (Table 1). This observation also supports the finding of increased preservation of
421 cutin, suberin, and long-chain lipids in the O horizon. The increased plant cutin, suberin, and long-
422 chain lipids in the A horizon were not captured by the alkyl C in NMR spectra likely because ^{13}C
423 NMR spectra do not detect subtle changes to SOC whereas targeted biomarker analyses are more
424 sensitive for measuring SOC composition (Simpson and Simpson 2012).

425 Polymeric carbohydrates, such as cellulose, are the most abundant form of plant inputs
426 (Kögel-Knabner 2002; Bianchi 2011). ^{13}C NMR analysis showed that the *O*-alkyl C (mainly
427 derived from cellulose) decreased with N fertilization for all horizons (Table 1). The decreased
428 cellulose-derived *O*-alkyl C may be explained by the N-stimulated cellulase enzyme activity and
429 selectively accelerated cellulose degradation (Hobbie et al. 2012; Thomas et al. 2012). Similarly,
430 the simple carbohydrates (including mannose, glucose, sucrose, and trehalose) did not increase
431 significantly with N fertilization (Fig. 6). This is likely due to accelerated sugar degradation with
432 N fertilization and is consistent with the observed *O*-alkyl C degradation. However, different from
433 the *O*-alkyl C, the sugars were slightly lower in the A horizon and slightly higher in B horizon. In
434 the A horizon, these changes coincide with the highest degree of stress in bacteria indicated by the

435 PLFA stress ratios (Fig. 5) as well as a significant decrease in PLFA and microbial short-chain
436 lipids storage (Table 2). Thus, the lack of favorable microbial substrates, such as cellulose and
437 related carbohydrates, in the A horizon may also be responsible for the large microbial suppression
438 in this horizon (Billings and Ziegler 2008; Watzinger 2015; Müller et al. 2017). The small increase
439 in sugar storage in the B horizon with N fertilization may also be due to leaching of these
440 compounds from the O and A soil horizons. Overall, carbohydrates, either in polymeric or simple
441 form, displayed the least accrual with N fertilization in all studied plant-derived SOC components.
442
443 Implications for biogeochemical processes and ecosystem services
444 Here, we demonstrate that the 22 years of N fertilization reduced the microbial processing
445 and altered the biogeochemistry of several specific SOC components. The component-specific
446 SOC accrual did not directly link to the molecular size but appeared to associate with SOC
447 recalcitrance or antimicrobial properties and sources. We found higher contributions of relatively
448 stable or antimicrobial plant-derived compounds (e.g. steroids, lignin, cutin, long-chain lipids, and
449 suberin) over microbial-derived compounds (e.g., PLFAs and short-chain lipids) and relatively
450 labile plant-derived compounds (e.g., carbohydrates). A recent study reported that N fertilization
451 increased soil organic matter accumulation without altering its biochemical composition (Zak et
452 al. 2017). Although we used more detailed molecular techniques to investigate the composition of
453 SOC with long-term N fertilization, the disparity in reports also highlights the varying responses
454 of different forest ecosystems. For example, Gallardo and Schlesinger (1994) reported increases
455 in microbial biomass with short-term N fertilization but also identified the importance of other
456 limiting nutrients, such as phosphorus. Additionally, variations in accrual across SOC
457 components may partially explain why SOC from different forests, which are expected to vary in

458 biochemical composition due to differences in tree species composition, forest age and disturbance
459 history, soil characteristics, and climate, display inconsistent total SOC responses to N fertilization
460 (Janssens et al. 2010; Lu et al. 2011; Frey et al. 2014; Yue et al. 2016).

461 Anthropogenically-accelerated global N deposition in forests will certainly continue in the
462 coming decades (Lamarque 2005) resulting in a suppression of microbial biomass and shifts in
463 microbial community composition that will subsequently hamper microbial processing of SOC
464 and slow down C cycling. Increases in forest soil C might be perceived as a benefit, given the large
465 amount of C stored in forest soils, and that small percentage changes in storage rates will translate
466 to meaningful global C budgetary contributions. However, concomitant with SOC storage, reduced
467 decomposition will alter additional variables. For example, nutrient release from soil organic
468 matter will decrease, which will decrease soil fertility thus altering ecosystem productivity and
469 forest biomass C sequestration. Overall, long-term N deposition shifts the fundamental
470 biogeochemical cycling via not only alteration in SOC quantity but also its molecular components.
471 Alteration of SOC quality may influence additional biogeochemical processes. For example,
472 accumulation of the antimicrobial and recalcitrant SOC components is unfavorable to soil
473 microbiota. Furthermore, altered accrual of specific SOC components will make the response of
474 forests to continued N deposition more difficult to predict given that these components respond
475 uniquely and precisely to changes in climate variables (e.g., temperature and precipitation (Pisani
476 et al. 2015; Greaver et al. 2016)) and may react differently with inorganic soil components (e.g.,
477 minerals and nutrients). This work highlights critical linkages between C and N cycles and
478 exemplifies that N deposition can alter the rates of organic matter decomposition, thus influencing
479 a host of important ecological processes that control forest productivity. Additionally, we
480 demonstrate that quantifying global C budgets needs to consider dynamic environmental changes

481 that will alter rates of C processing and storage over time, and that concerted efforts to manage
482 soil C, such as through N fertilization, need to be evaluated more holistically.
483
484 **Acknowledgements**
485 This research was supported by the Natural Sciences and Engineering Research Council (NSERC)
486 of Canada via a Discovery Grant (#2015-05760) and a Discovery Accelerator Supplement
487 (#478038-15) to M.J.S. We sincerely thank Lori vandenEnden, Zhangliu Du, Sam Reese, Ivy Ryan,
488 and Allegheny College for field, laboratory, and financial assistance.
489
490 **References**
491 Aber J, McDowell W, Nadelhoffer K, et al (1998) Nitrogen saturation in temperate forest
492 ecosystems. Bioscience 48:921–934.
493 Adamczyk S, Adamczyk B, Kitunen V, Smolander A (2015) Monoterpenes and higher terpenes
494 may inhibit enzyme activities in boreal forest soil. Soil Biol Biochem 87:59–66
495 Allison SD, Czimczik CI, Treseder KK (2008) Microbial activity and soil respiration under
496 nitrogen addition in Alaskan boreal forest. Glob Chang Biol 14:1156–1168.
497 Angst G, Heinrich L, Kögel-Knabner I, Mueller CW (2016) The fate of cutin and suberin of
498 decaying leaves, needles and roots - Inferences from the initial decomposition of bound fatty
499 acids. Org Geochem 95:81–92.
500 Baldock JA, Oades JM, Waters AG, et al (1992) Aspects of the chemical structure of soil organic
501 materials as revealed by solid-state ^{13}C NMR spectroscopy. Biogeochemistry 16:1–42
502 Bhatnagar JM, Peay KG, Treseder KK (2018) Litter chemistry influences decomposition through
503 activity of specific microbial functional guilds. Ecol Monogr 88:429–444.
504 Bianchi TS (2011) The role of terrestrially derived organic carbon in the coastal ocean: a changing
505 paradigm and the priming effect. Proc Natl Acad Sci 108:19473–19481
506 Billings SA, Ziegler SE (2008) Altered patterns of soil carbon substrate usage and heterotrophic
507 respiration in a pine forest with elevated CO_2 and N fertilization. Glob Chang Biol 14:1025–
508 1036.

509 Bossio DA, Scow KM (1998) Impacts of carbon and flooding on soil microbial communities:
510 phospholipid fatty acid profiles and substrate utilization patterns. Microb Ecol 35:265–278.
511 Bowden RD, Deem L, Plante AF, et al (2014) Litter input controls on soil carbon in a temperate
512 deciduous forest. Soil Sci Soc Am J 78:S66–S75
513 Bowden RD, Rullo G, Stevens GR, Steudler PA (2000) Soil fluxes of carbon dioxide, nitrous oxide,
514 and methane at a productive temperate deciduous forest. J Environ Qual 29:268–276
515 Bowden, R.D., Steudler PA, Melillo JM and Aber JD. 1990. Annual nitrous oxide fluxes from
516 temperate forest soils in the northeastern United States. J. Geophys. Res. 95:13997-14005.
517 Chan ASK, Steudler PA, Bowden RD, et al (2005) Consequences of nitrogen fertilization on soil
518 methane consumption in a productive temperate deciduous forest. Biol Fertil Soils 41:182–
519 189.
520 Conte P, Spaccini R, Piccolo A (2004) State of the art of CPMAS 13C-NMR spectroscopy applied
521 to natural organic matter. Prog Nucl Magn Reson Spectrosc 44:215–223
522 Crow SE, Lajtha K, Filley TR, et al (2009) Sources of plant-derived carbon and stability of organic
523 matter in soil: implications for global change. Glob Chang Biol 15:2003–2019
524 Dria KJ, Sachleben JR, Hatcher PG (2002) Solid-State Carbon-13 Nuclear Magnetic Resonance
525 of Humic Acids at High Magnetic Field Strengths. J Environ Qual 31:393–401.
526 Du E, de Vries W, Galloway JN, et al (2014) Changes in wet nitrogen deposition in the United
527 States between 1985 and 2012. Environ Res Lett 9:095004 (8 pages).
528 Eswaran H, Vandenberg E, Reich P (1993) Organic-carbon in soils of the world. Soil Sci Soc Am
529 J 57:192–194.
530 Feng X, Simpson MJ (2009) Temperature and substrate controls on microbial phospholipid fatty
531 acid composition during incubation of grassland soils contrasting in organic matter quality.
532 Soil Biol Biochem 41: 804-812.
533 Feng X, Simpson AJ, Schlesinger WH, Simpson MJ (2010) Altered microbial community structure
534 and organic matter composition under elevated CO_2 and N fertilization in the duke forest.
535 Glob Chang Biol 16:2104–2116.
536 Feng X, Simpson MJ (2009) Temperature and substrate controls on microbial phospholipid fatty
537 acid composition during incubation of grassland soils contrasting in organic matter quality.
538 Soil Biol Biochem 41:804–812.
539 Frey SD, Ollinger S, Nadelhoffer K, et al (2014) Chronic nitrogen additions suppress

decomposition and sequester soil carbon in temperate forests. Biogeochemistry 121:305–316
Frostegård A, Bååth E (1996) The use of phospholipid fatty acid analysis to estimate bacterial and fungal biomass in soil. Biol Fertil Soils 22:59–65
Gallardo A, Schlesinger WH (1994) Factors limiting microbial biomass in the mineral soil and forest floor of a warm-temperate forest. Soil Biol Biochem 26:1409–1415.
Gallo ME, Lauber CL, Cabaniss SE, et al (2005) Soil organic matter and litter chemistry response to experimental N deposition in northern temperate deciduous forest ecosystems. Glob Chang Biol 11:1514–1521.
Galloway JN, Townsend AR, Erisman JW, et al (2008) Transformation of the nitrogen cycle: recent trends, questions, and potential solutions. Science 320:889–892.
Greaver TL, Clark CM, Compton JE, et al (2016) Key ecological responses to nitrogen are altered by climate change. Nat Clim Chang 6:836–843.
Hatton PJ, Kleber M, Zeller B, et al (2012) Transfer of litter-derived N to soil mineral-organic associations: evidence from decadal ^{15}N tracer experiments. Org Geochem 42:1489–1501.
Hedges JI, Blanchette RA, Weliky K, Devol AH (1988) Effects of fungal degradation on the CuO oxidation products of lignin: a controlled laboratory study. Geochim Cosmochim Acta 52:2717–2726.
Hobbie SE, Eddy WC, Buyarski CR, et al (2012) Response of decomposing litter and its microbial community to multiple forms of nitrogen enrichment. Ecol Monogr 82:389–405.
Janssens IA, Dieleman W, Luyssaert S, et al (2010) Reduction of forest soil respiration in response to nitrogen deposition. Nat Geosci 3:315–322.
Kögel-Knabner I (2002) The macromolecular organic composition of Plant and microbial residues as inputs to soil organic matter. Soil Biol Biochem 34:139–162.
Lamarque J-F (2005) Assessing future nitrogen deposition and carbon cycle feedback using a multimodel approach: Analysis of nitrogen deposition. J Geophys Res 110:D19303.
Lehmann J, Kleber M (2015) The contentious nature of soil organic matter. Nature 528:60–8. d
Li XG, Jia B, Lv J, et al (2017) Nitrogen fertilization decreases the decomposition of soil organic matter and plant residues in planted soils. Soil Biol Biochem 112:47–55.
Li Y, Schichtel BA, Walker JT, et al (2016) Increasing importance of deposition of reduced nitrogen in the United States. Proc Natl Acad Sci 113:5874–5879.
Liu J, Wu N, Wang H, et al (2016a) Nitrogen addition affects chemical compositions of plant

571 tissues, litter and soil organic matter. Ecology 97:1796–1806.
572 Lu M, Zhou X, Luo Y, et al (2011) Minor stimulation of soil carbon storage by nitrogen addition:
573 a meta-analysis. Agric Ecosyst Environ 140:234–244.
574 Morrison EW, Frey SD, Sadowsky JJ, et al (2016) Chronic nitrogen additions fundamentally
575 restructure the soil fungal community in a temperate forest. Fungal Ecol 23:48–57.
576 Müller K, Marhan S, Kandeler E, Poll C (2017) Carbon flow from litter through soil
577 microorganisms: From incorporation rates to mean residence times in bacteria and fungi. Soil
578 Biol Biochem 115:187–196.
579 NADP (National Atmospheric Deposition Program), University of Wisconsin, Wisconsin State
580 Laboratory of Hygiene, http://nadp.slh.wisc.edu/NADP (accessed 11/9/2018).
581 Otto A, Shunthirasingham C, Simpson MJ (2005) A comparison of plant and microbial biomarkers
582 in grassland soils from the Prairie Ecozone of Canada. Org Geochem 36:425–448.
583 Otto A, Simpson MJ (2007) Analysis of soil organic matter biomarkers by sequential chemical
584 degradation and gas chromatography - Mass spectrometry. J Sep Sci 30:272 – 282.
585 Otto A, Simpson MJ (2006) Sources and composition of hydrolysable aliphatic lipids and phenols
586 in soils from western Canada. Org Geochem 37:385–407.
587 Pan Y, Birdsey RA, Fang J, et al (2011) A Large and Persistent Carbon Sink in the World's Forests.
588 Science (80-) 333:988–993.
589 Pardo LH, Robin-Abbott MJ, Fenn ME, et al (2015) Effects and Empirical Critical Loads of
590 Nitrogen for Ecoregions of the United States. Ecol Appl 21:129–169.
591 Peng Y, Guo D, Yang Y (2017) Global patterns of root dynamics under nitrogen enrichment. Glob
592 Ecol Biogeogr 26:102–114.
593 Pisani O, Frey SD, Simpson AJ, Simpson MJ (2015) Soil warming and nitrogen deposition alter
594 soil organic matter composition at the molecular-level. Biogeochemistry 123:391–409.
595 Preston CM, Trofymow JA, Sayer BG, Niu J (1997) ^{13}C nuclear magnetic resonance spectroscopy
596 with cross-polarization and magic-angle spinning investigation of the proximate-analysis
597 fractions used to assess litter quality in decomposition studies. Can J Bot 75:1601–1613.
598 Pries CEH, Castanha C, Porras RC, Torn MS (2017) The whole-soil carbon flux in response to
599 warming. Science (80-) 355:1420–1422.
600 Ramirez KS, Craine JM, Fierer N (2012) Consistent effects of nitrogen amendments on soil
601 microbial communities and processes across biomes. Glob Chang Biol 18:1918–1927.

Schmidt MWI, Knicker H, Hatcher PG, Kögel-Knabner I (1997) Improvement of ^{13}C and ^{15}N CPMAS NMR spectra of bulk soils, particle size fractions and organic material by treatment with 10% hydrofluoric acid. Eur J Soil Sci 48:319–328.

Schmidt MWI, Torn MS, Abiven S, et al (2011) Persistence of soil organic matter as an ecosystem property. Nature 478:49–56.

Simpson MJ, Simpson AJ (2012) The chemical ecology of soil organic matter molecular constituents. J Chem Ecol 38:768–784.

Smania EFA, Delle Monache F, Smania A, et al (2003) Antifungal activity of sterols and triterpenes isolated from Ganoderma annulare. Fitoterapia 74:375–377.

Sollins P, Kramer MG, Swanston C, et al (2009) Sequential density fractionation across soils of contrasting mineralogy: evidence for both microbial- and mineral-controlled soil organic matter stabilization. Biogeochemistry 96:209–231.

Sollins P, Swanston C, Kleber M, et al (2006) Organic C and N stabilization in a forest soil: Evidence from sequential density fractionation. Soil Biol Biochem 38:3313–3324.

Theuerl S, Dorr N, Guggenberger G, et al (2010) Response of recalcitrant soil substances to reduced N deposition in a spruce forest soil: integrating laccase-encoding genes and lignin decomposition. Fems Microbiol Ecol 73:166–177.

Thomas DC, Zak DR, Filley TR (2012) Chronic N deposition does not apparently alter the biochemical composition of forest floor and soil organic matter. Soil Biol Biochem 54:7–13.

Treseder KK (2008) Nitrogen additions and microbial biomass: a meta-analysis of ecosystem studies. Ecol Lett 11:1111–1120.

Tritton LM, Hornbeck JW (1982) Biomass equations for major tree species of the Northeast. US Department of Agriculture, Forest Service, Northeastern Forest Experiment Station.

Vet, R., R.S. Artz, S. Carou, M. Shaw, C.U. Ro, W. Aas, A. Baker, V.C. Bowersox, F. Dentener, C. Galy-Lacaux, A. Hou, J.J. Pienaar, R. Gillett, M.C. Forti, S. Gromov, H. Hara, T. Khodzher, N.M. Mahowald, S. Nickovic, P.S.P. Rao, and N.W. Reid. 2014. A global assessment of precipitation chemistry and deposition of sulfur, nitrogen, sea salt, base cations, organic acids, acidity and pH, and phosphorus. Atmos. Environ. 93: 3–100. doi: 10.1016/j.atmosenv.2013.10.060.

631 Waldner, P., A. Marchetto, A. Thimonier, M. Schmitt, M. Rogora, O. Granke, V. Mues, K. Hansen,
632 G. Pihl Karlsson, D. Žlindra, N. Clarke, A. Verstraeten, A. Lazdins, C. Schimming, C.
633 Iacoban, A.J. Lindroos, E. Vanguelova, S. Benham, H. Meesenburg, M. Nicolas, A.
634 Kowalska, V. Apuhtin, U. Napa, Z. Lachmanová, F. Kristoefel, A. Bleeker, M. Ingerslev, L.
635 Vesterdal, J. Molina, U. Fischer, W. Seidling, M. Jonard, P. O'Dea, J. Johnson, R. Fischer,
636 and M. Lorenz. 2014. Detection of temporal trends in atmospheric deposition of inorganic
637 nitrogen and sulphate to forests in Europe. Atmos. Environ. 95: 363–374. doi:
638 10.1016/j.atmosenv.2014.06.054.

639 Wang J-J, Pisani O, Lin LH, et al (2017) Long-term litter manipulation alters soil organic matter
640 turnover in a temperate deciduous forest. Sci Total Environ 607–608: 865-875.

641 Watzinger A (2015) Microbial phospholipid biomarkers and stable isotope methods help reveal
642 soil functions. Soil Biol Biochem 86:98–107.

643 Wu NN, Filley TR, Bai E, et al (2015) Incipient changes of lignin and substituted fatty acids under
644 N addition in a Chinese forest soil. Org Geochem 79:14–20.

645 Xia M, Talhelm AF, Pregitzer KS (2017) Chronic nitrogen deposition influences the chemical
646 dynamics of leaf litter and fine roots during decomposition. Soil Biol Biochem 112:24–34.

647 Yue K, Peng Y, Peng C, et al (2016) Stimulation of terrestrial ecosystem carbon storage by
648 nitrogen addition: a meta-analysis. Sci Rep 6:19895.

649 Zak DR, Freedman ZB, Upchurch RA, et al (2017) Anthropogenic N deposition increases soil
650 organic matter accumulation without altering its biochemical composition. Glob Chang Biol
651 23:933–944.

652 Zelles L, Bai QY, Rackwitz R, et al (1995) Determination of phospholipid- and
653 lipopolysaccharide-derived fatty acids as an estimate of microbial biomass and community
654 structures in soils. Biol Fertil Soils 19:115–123.

Table 1: Total carbon (C) and nitrogen (N) contents and organic matter composition of control and N-fertilized soil samples measured by solid-state ^{13}C nuclear magnetic resonance spectroscopy. Significant differences between treatments within each horizon at $P<0.1$ are indicated with an asterisk.

Soil horizon	**Treatment**	**Total C (%)**	**Total N (%)**	**Alkyl C (0-50 ppm)**	***O*-alkyl C (50-110 ppm)**	**Aromatic & phenolic C (110-165 ppm)**	**Carboxyl & carbonyl C (165-210 ppm)**	**Alkyl/*O*-alkyl C ratio**
O horizon	Control	22.20±3.27*	1.45±0.20	27%	47%	15%	11%	0.57
	N-fertilized	30.24±2.47*	1.89±0.14	29%	44%	16%	11%	0.66
A horizon	Control	6.77±1.38*	0.52±0.08	35%	39%	14%	12%	0.90
	N-fertilized	10.06±0.98*	0.70±0.07	35%	38%	15%	12%	0.92
B horizon	Control	3.34±0.37	0.27±0.02	37%	38%	13%	12%	0.97
	N-fertilized	3.65±0.20	0.26±0.01	37%	37%	14%	12%	1.00

Table 2. Summary of changes in average storage (mass per square meter of soil) of carbon and organic compounds in soils with N fertilization. "~" indicates minor alteration within ±10%; "–" and "––" show >10% and >50% decreases from Control, respectively; "+" and "++" show >10% and >50% increases from Control, respectively; *, and ** indicate statistically significant differences at $P<0.1$ and $P<0.05$, respectively.

Parameters*	Unit	Indicator for	Total	O horizon	A horizon	B horizon
Carbon storage	kg m^{-2}	Total C abundance	+	++**	+	~
Phospholipid fatty acids (PLFAs)						
Gram-negative bacterial PLFAs	g m^{-2}	Bacterial biomass	–**	–	––**	–
Gram-positive bacterial PLFAs	g m^{-2}	Bacterial biomass	–**	–	––**	~
Fungal PLFA	g m^{-2}	Fugal biomass	–	~	––*	+
Total PLFAs	g m^{-2}	Microbial biomass	–**	–	––**	~
Solvent-extractable compounds						
Short-chain lipids (<C_{20})	g m^{-2}	Microbial lipids	~	~	–	+
Long-chain lipids (≥C_{20})	g m^{-2}	Plant lipids	+	++**	+	+
Plant-derived steroids	g m^{-2}	Plant-derived steroids	++**	++**	++	++
Sugars	g m^{-2}	Simple sugars	~	+	–	+*
Hydrolysable lipids						
Cutin-derived compounds	g m^{-2}	Extractable cutin compounds	++	++**	++	–
Suberin-derived compounds	g m^{-2}	Extractable suberin compounds	+	++**	+	–
Sum of suberin- and cutin-derived compounds	g m^{-2}	Extractable suberin and cutin compounds	+	++**	+	–
Lignin-derived phenols						
Total lignin-derived phenols (VSC)	g m^{-2}	Extractable lignin phenols	++**	++**	++	+

*Gram-negative bacterial PLFAs include: 16:1ω7*c*, *cy*17:0, 18:1ω7*c* and *cy*19:0.
Gram-positive bacterial PLFAs include: *i*14:0, *i*15:0, *a*15:0, *i*16:0, *a*16:0, *i*17:0 and *a*17:0.
Fugal PLFA is 18:2ω6,9*c*.
Short-chain (<C_{20}) and long-chain (≥C_{20}) lipids include: C_{16}-C_{33} *n*-alkanes, *n*-alkanols, and *n*-alkanoic acids.
Plant-derived steroids include: β-sitosterol, stigmasterol, sitosterone, stigmasta-3,5-dien-7-one, and campesterol.
Sugars include: mannose, glucose, sucrose, and trehalose.
Cutin-derived compounds include: short-chain mid-chain-hydroxy acids, C_{16} mono- and dihydroxy acids and dioic acids.
Suberin-derived compounds include: long-chain ω-hydroxyalkanoic and dioic acids, and 9,10-epoxy-ω-hydroxy C_{18} acid.
Total lignin-derived phenols include: vanillyl (vanillic acid, acetovanillone, vanillin), syringyl (syringic acid, acetosyringone, syringaldehyde), and cinnamyl (*p*-coumaric acid, ferulic acid) phenols.

Figure Captions

Fig. 1. Soil carbon storage in control and N-fertilized plots (mean ± standard error; n=6). Percentages in figures show percent change compared to the control. Significant difference between treatment and control at $P<0.05$ is indicated with an asterisk.

Fig. 2. Mineral soil horizons density fractions of control and N-fertilized plots (mean ± standard error; n=6). Significant differences between treatments within each horizon at $P<0.05$ are indicated with an asterisk.

Fig. 3. Litterfall, aboveground production, and standing fine root (0-1 mm diameter) mass in control and N-fertilized plots (mean ± standard error; n=3 plots per treatment; litterfall flux in each plot is the average of data from two 1 m^2 collectors; fine root mass in each plot is the average of data from three 15×15-cm-area soil blocks). Significant difference between treatment and control at $P<0.05$ is indicated with an asterisk.

Fig. 4. Percent mass remaining of leaf litter samples after one year of *in-situ* litter decomposition at control and N-fertilized plots (mean ± standard error; n=12). Mixed leaf litter included 53.8% sugar maple (*Acer saccharum* Marshall), 29.5% black cherry (*Prunus serotina* Ehrh.), and 16.7% American beech (*Fagus grandifolia* Ehrh.) leaf litter. Significant differences between treatment and control at $P<0.05$ are indicated with asterisks.

Fig. 5. Phospholipid fatty acid (PLFA) concentrations and stress ratios in control and N-fertilized plots (mean ± standard error; n=6). Significant differences between treatment and control at $P<0.05$ are indicated with asterisks.

Fig. 6. Changes in the storage of plant-derived soil organic carbon components (in g m^{-2} soil) in control and N-fertilized plots (mean ± standard error; n=6). Percentages in figures are the percent change compared to the control. Significant differences between treatment and control at $P<0.05$ are indicated with asterisks. Plant-derived biopolymer compounds are underlined. Detailed quantification of specific organic matter compounds is provided in the Supplementary Materials.

Fig. 1.

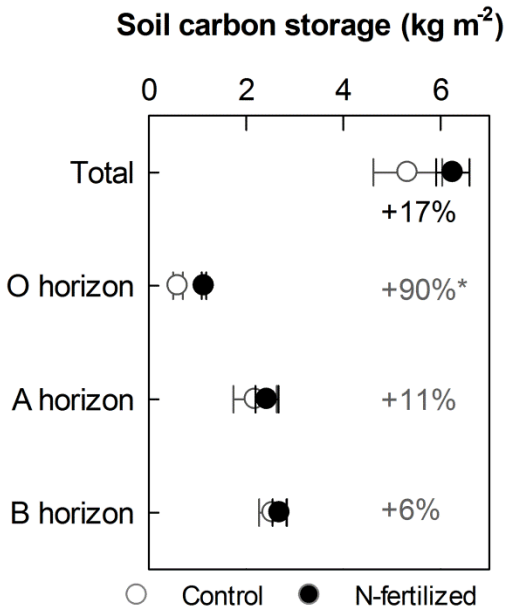
Soil carbon storage (kg m-2)
0
2
4
6
Total
+17%
O horizon
+90%*
A horizon
+11%
B horizon
+6%
Control
N-fertilized

Fig. 2.

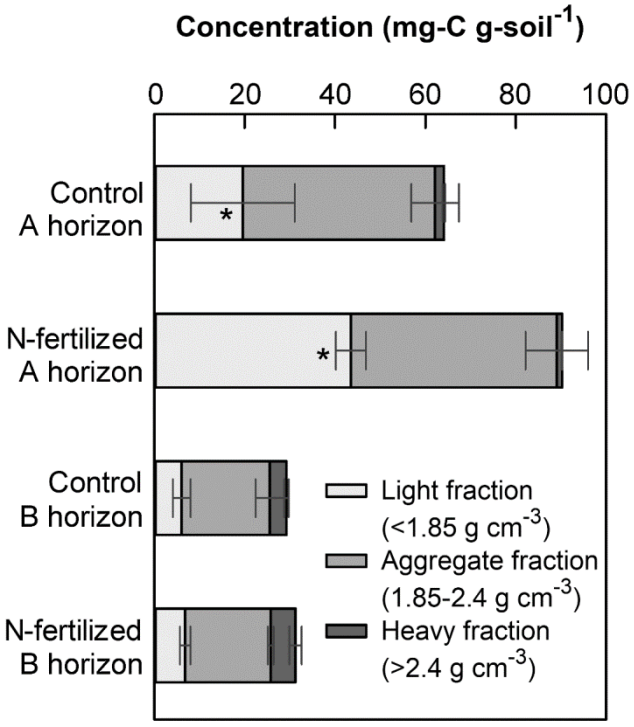
Concentration (mg-C g-soil-1)
0
20
40
60
80
100
Control
A horizon
N-fertilized
A horizon
Control
B horizon
N-fertilized
B horizon
*
*
Light fraction
(<1.85 g cm-3)
Aggregate fraction
(1.85-2.4 g cm-3)
Heavy fraction
(>2.4 g cm-3)

Fig. 3.

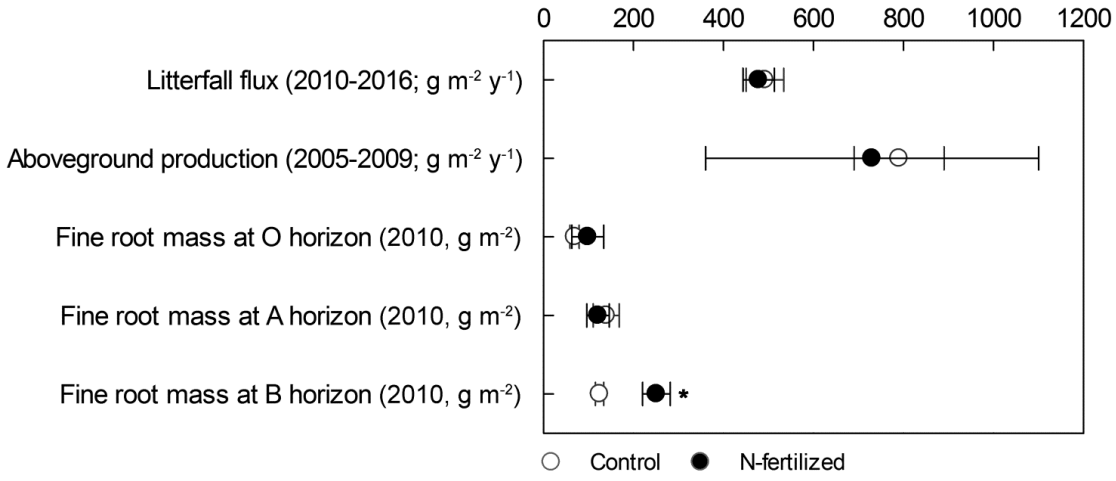
0
200
400
600
800
1000
1200
Litterfall flux (2010-2016; g m-2 y-1)
Aboveground production (2005-2009; g m-2 y-1)
Fine root mass at O horizon (2010, g m-2)
Fine root mass at A horizon (2010, g m-2)
Fine root mass at B horizon (2010, g m-2)
*
Control
N-fertilized

Fig. 4.

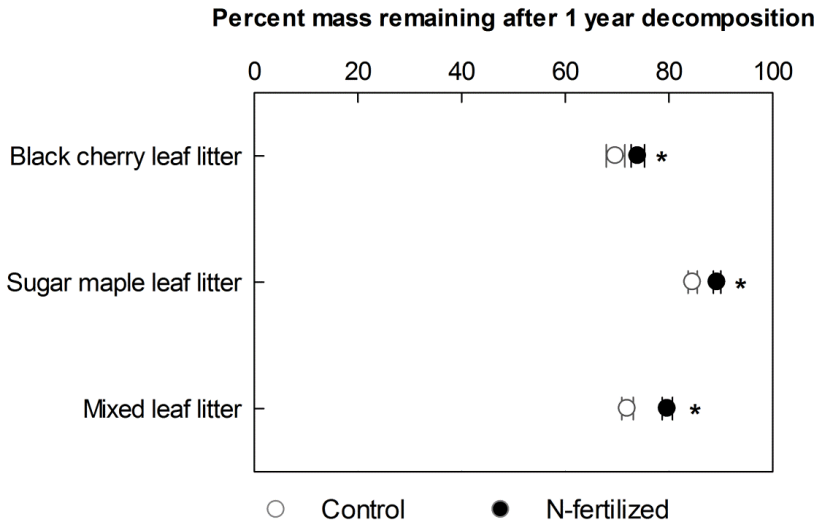
Percent mass remaining after 1 year decomposition
0
20
40
60
80
100
Black cherry leaf litter
Sugar maple leaf litter
Mixed leaf litter
*
*
*
Control
N-fertilized

Fig. 5.

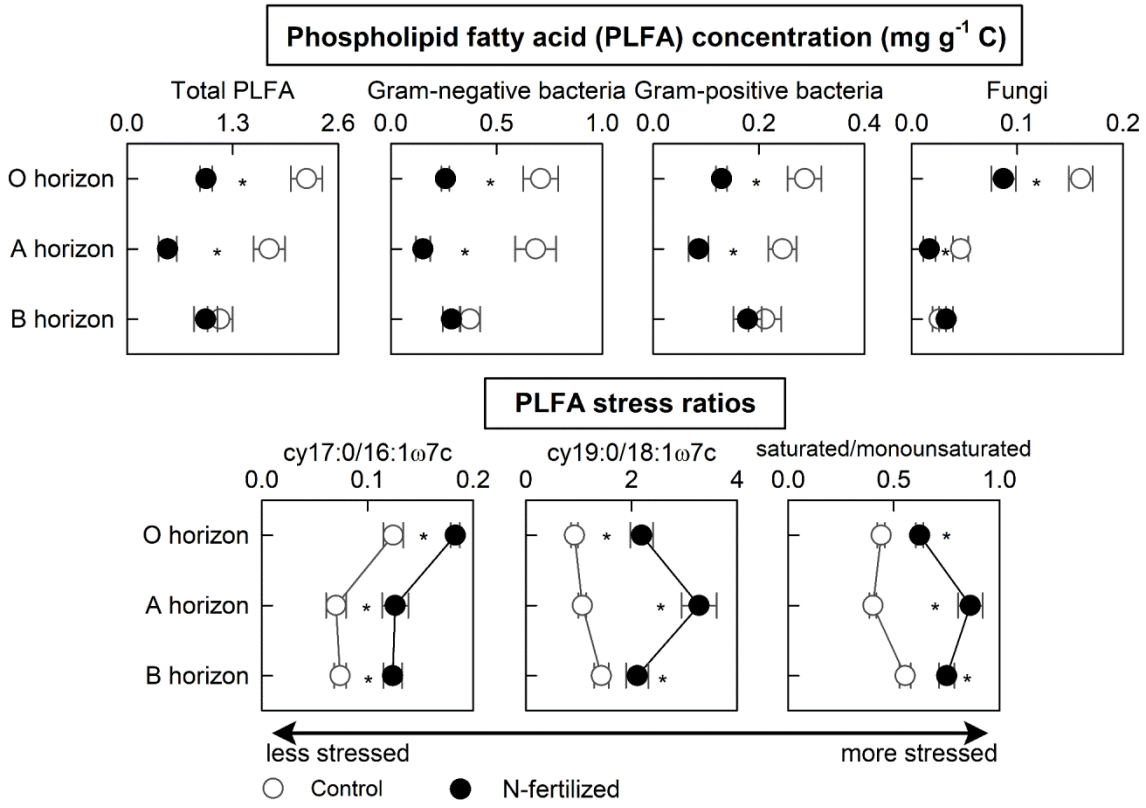
Phospholipid fatty acid (PLFA) concentration (mg g-1 C)
Total PLFA
Gram-negative bacteria
Gram-positive bacteria
Fungi
0.0
1.3
2.6
0.0
0.5
1.0
0.0
0.2
0.4
0.0
0.1
0.2
O horizon
A horizon
B horizon
PLFA stress ratios
cy17:0/16:1ω7c
cy19:0/18:1ω7c
saturated/monounsaturated
0.0
0.1
0.2
0
2
4
0.0
0.5
1.0
O horizon
A horizon
B horizon
less stressed
more stressed
Control
N-fertilized

Fig. 6.

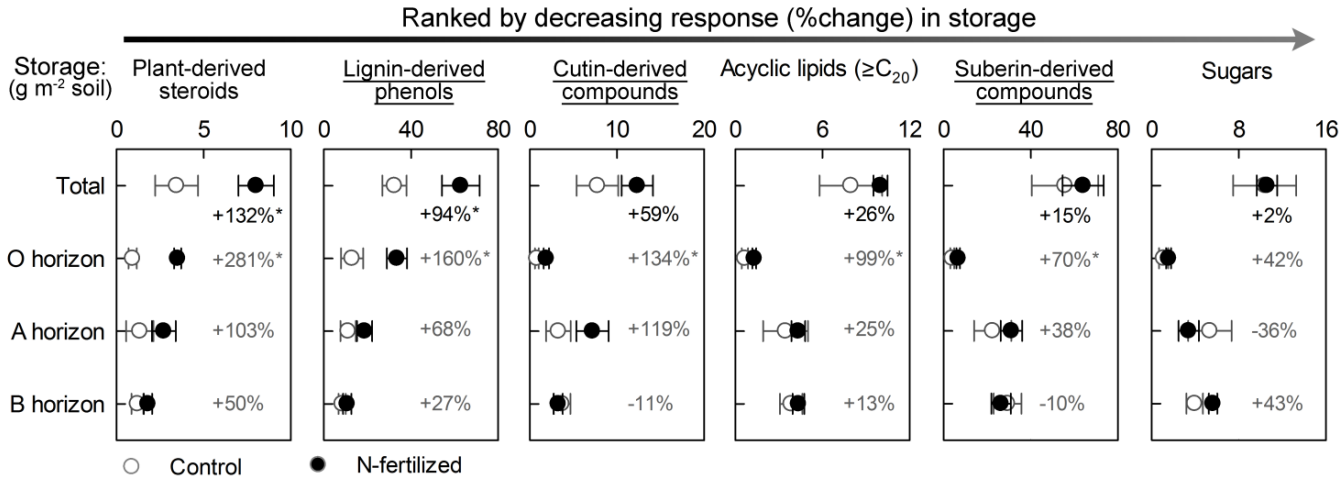
Ranked by decreasing response (%change) in storage
Storage: (g m-2 soil)
Plant-derived steroids
Lignin-derived phenols
Cutin-derived compounds
Acyclic lipids (≥C20)
Suberin-derived compounds
Sugars
0 5 10
0 40 80
0 10 20
0 6 12
0 40 80
0 8 16
Total
O horizon
A horizon
B horizon
+132%*
+281%*
+103%
+50%
+94%*
+160%*
+68%
+27%
+59%
+134%*
+119%
-11%
+26%
+99%*
+25%
+13%
+15%
+70%*
+38%
-10%
+2%
+42%
-36%
+43%
Control
N-fertilized